The baseline capability of the cosmogenic neutrino search with IceCube

THE ICECUBE COLLABORATION[1]
[1]*See the special section in these proceedings*

Abstract: We present the expected baseline sensitivity of the IceCube detector to cosmogenic neutrinos produced through the GZK process. Data from the partially completed IceCube detector have previously been searched for such highly energetic ($\geq 10^6$ GeV) neutrinos. With the completion of the detector in December 2010 and the full operation having started in May 2011, IceCube's sensitivity to these neutrinos is significantly improved from previous studies. We calculate the expected sensitivity in the search of cosmogenic (GZK) neutrinos using a Monte Carlo simulation of the completed IceCube detector and the selection criteria developed in the previous analysis. The sensitivity for a diffuse flux of cosmic neutrinos with an E^{-2} spectrum in the central 90% energy range 300 TeV to 2 EeV is expected to be at a level of $E^2\phi_{\nu_e+\nu_\mu+\nu_\tau} \leq 1.3 \times 10^{-8}$ GeVcm^{-2} sec^{-1}sr^{-1} with one year of operation. The corresponding differential sensitivity is also presented.

Corresponding author: Aya Ishihara[2] (*aya@hepburn.s.chiba-u.ac.jp*)
[2]*Chiba University, Yayoi-cho 1-33, Inage-ku, Chiba, Chiba, 26-0045 Japan*

DOI: 10.7529/ICRC2011/V02/0773

Keywords: IceCube, cosmogenic neutrinos, GZK mechanism

1 Cosmogenic neutrinos with IceCube

Cosmogenic neutrinos are produced in the interactions of the highest energy cosmic-rays with the cosmic-microwave background (CMB) photons (the GZK process [1, 2]) and subsequent charged pion decays [3]. These cosmogenic (GZK) neutrinos are one of the most promising messengers from the high energy, distant universe beyond PeV energies. They may provide us with direct evidence of the highest energy cosmic ray sources unlike the other messengers, such as gamma-rays and cosmic-rays, which experience interactions with the CMB and/or galactic and extra-galactic magnetic fields.

IceCube is a cubic kilometer scale deep underground Cherenkov neutrino detector at the South Pole. The IceCube detector construction was completed in December 2010. The IceCube array [4] comprises 5160 optical sensors on 86 cables, called strings, over a 1 km^3 fiducial volume of ice at a depth of 1450 m $\sim$ 2450 m. In 2008-2009, 40 out of 86 cables were deployed and taking data with an approximate fiducial volume of 0.5 km^3. Results from the cosmogenic neutrino search with the half-completed configuration of IceCube [5] generated the best published limit to date on the neutrino fluxes above 1 PeV and up to 10 EeV.

In this proceeding, we present the expected sensitivity of the completed IceCube detector to cosmogenic neutrino fluxes calculated using a Monte Carlo simulation. The signal discrimination methods are based on the selection criteria utilized in the 2008-2009 data analysis with the partially instrumented 40-string detector [5].

In the energy region above 1 PeV, the primary variable used to discriminate signal from background is the energy of

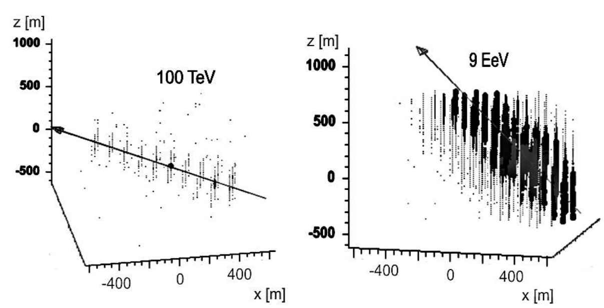

Figure 1: Simulated single muon events in IceCube. Left panel shows a 100 TeV muon track representing the conventional event while the right panel indicates a 9 EeV muon EHE event. Circles denote optical sensors with more than one photo-electron signal recorded. The size of the circles represents the number of photo-electrons. Axes are distances in meters from the center of the IceCube detector array.

the particles. This is because the conventional atmospheric neutrino and muon background spectra are proportional to $E^{-3.7}$ or steeper, while signal spectra follow $E^{-1} \sim E^{-2}$ in the energy region considered. Since the amount of energy deposited in the form of Cherenkov photons by the neutrino-induced charged particles in the detector is highly correlated with their energy, the extremely-high energy neutrino signal stands out against the atmospheric muon and neutrino background because of the much higher light deposition. The total number of photo-electrons (NPE) recorded in an event is used as the main distinctive feature to separate signal from background. Figure 1 illustrates the difference in the energy deposition in the IceCube detector from a background-like 100 TeV muon and a signal-like 9 EeV muon.

2 Event selection

The primary background in this analysis is muon bundles made up of large numbers of muons produced by high energy cosmic-ray interactions in the atmosphere dominating the downward-going directions. Because of the high multiplicity number, these events also leave a large amount of Cherenkov photons in IceCube. This background was simulated with the CORSIKA air-shower simulation package version 6.720 [6] with the SIBYLL 2.1 [7] hadronic interaction model. Cosmic-ray interactions assuming pure proton and iron primary compositions in the energy region between 10^5 and 10^{11} GeV were simulated. EHE neutrino signal events with energies between 10^5 and 10^{11} GeV from several flux models were simulated using the JULIeT package [12]. The cosmogenic neutrino induced tracks are most likely to have a near horizontal slightly downward-going geometry with falling distributions towards both vertically upward-going and downward-going directions due to the neutrino absorption in the Earth.

The simulated high energy events are divided into the shallow and deep event samples to take the difference in the optical properties of ice into account. The "depth" of the event is defined by the vertical position of the brightest photo-electron signal. The final background discrimination is performed using different sets of variables for the shallow and deep events as described in Ref. [5]. Figure 2 shows the event distributions in the planes of cos θ vs NPE for the shallow events and $\Delta t_{\mathrm{LN-E}}$ vs NPE for the deep events. Here θ is the reconstructed zenith angle of the event and $\Delta t_{\mathrm{LN-E}}$ is the time interval between the earliest (E) and the brightest (LN, largest NPE) photo-electron signal in the event. A clear separation between the signal and background can be observed. Reference [5] further describes the variables and compares the experimental and simulated event distributions. The straight lines and the quarter-elliptical shape show the applied NPE threshold value as a function of cos θ and $\Delta t_{\mathrm{LN-E}}$, respectively. The boundaries are set such that the background expectation from cosmic-rays of an assumed pure iron primary is 0.1 events per year. For a pure proton case the background events are estimated to be at least a factor of 5 reduced from the current estimate of the background event numbers. This selection enhances the discovery potential of IceCube, which with a signal-to-background ratio of around 10 becomes quite robust against large unknown systematics uncertainties in the background estimate.

3 IceCube sensitivity beyond a PeV

The quasi-differential model-independent sensitivity of the IceCube detector at 90% CL per energy decade for neutrino fluxes above 10^{15} eV (1 PeV) is shown in Fig. 3 assuming full standard neutrino mixing. The corresponding sensitivity for a diffuse flux of cosmic neutrinos with an E^{-2} spectrum in the central 90% energy range from 300 TeV to 2 EeV is calculated to be $E^2\phi_{\nu_e+\nu_\mu+\nu_\tau} \leq 1.3\times10^{-8}\ \mathrm{GeVcm^{-2}\ sec^{-1}sr^{-1}}$ with one year of observation. The improvement of the sensitivity from the analysis of the data taken with the half completed IceCube [5] is approximately a factor of two.

Table 1 gives the event rates for several model fluxes of cosmogenic neutrinos assuming cosmic-rays to be protons only. We expect 0.8 to 1.7 cosmogenic neutrino events per year, assuming moderate to strong cosmological source evolution models, while 0.11 background events are expected in the same time period.

The corresponding neutrino effective area is shown in Fig. 4. The neutrino effective area represents the surface

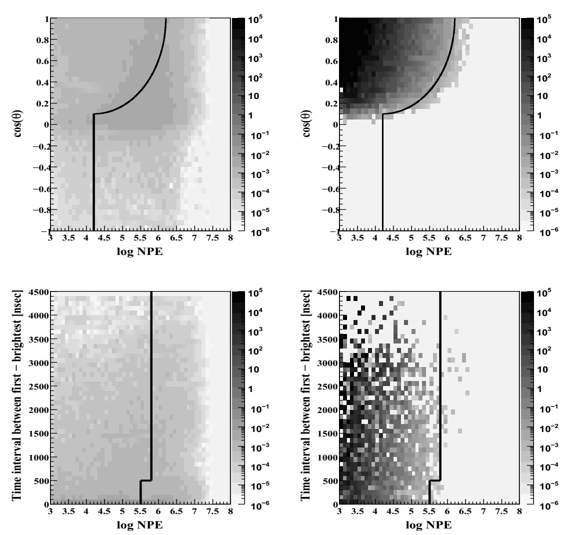

Figure 2: Event number distributions of the shallow (upper panels) and deep (lower panels) event samples in 365 days are shown for signal (left panels) and background (right panels) simulations. The signal distributions are from the cosmogenic neutrino model in Ref. [8] adding all three flavors of neutrinos. The background distributions are from CORSIKA-SIBYLL with iron primaries. The lines in each panel show the final selection criteria.

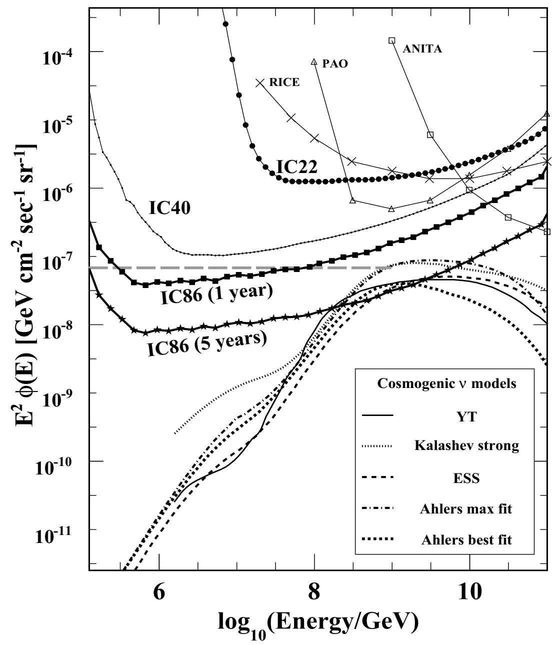

Figure 3: All flavor neutrino flux quasi-differential sensitivities of the IceCube detector after one year (filled squares) and five years (filled stars) of operations. Several model predictions (assuming primary protons) are shown for comparison: YT [8], Kalashev *et al.* (strong evolution) [9], ESS (Ω_Λ = 0.7) [10], Ahlers *et al.* (maximal), Ahlers *et al.* (the best fit, incorporating the Fermi-LAT bound) [11]. The gray dashed horizontal line indicates the Waxman-Bahcall flux bound with cosmological evolution [17]. Model fluxes are summed over all neutrino flavors, assuming standard neutrino oscillations. The model independent differential upper limits by other experiments are also shown for Auger (PAO) [13], RICE [14], ANITA [15], the previous IceCube results (2007-2008, IC22) [16], and (2008-2009, IC40) [5]. Limits from other experiments are converted to the all flavor limit assuming standard neutrino oscillation and a 90% CL per energy decade quasi-differential limit when necessary.

area of an equivalent detector if it were 100% efficient. For ν_μ and ν_τ, the areas exceed 10^3 m^2 at 10^9 GeV which is the main energy range in the IceCube cosmogenic neutrino search [5]. The present analysis is sensitive to all three neutrino flavors. Similarly the effective area near the IceCube detector can be defined as the area within which the neutrino induced muons and taus, or neutrinos are 100% detectable. They are shown in the right panel in Fig. 4. IceCube acts as a detector with effectively 50% larger volume than its actual size for neutrino-induced muons at 10^9 GeV. The effective area near the detector for the neutrinos interacting near or inside the detector (direct neutrino channel) is more than two orders of magnitude smaller than those for muons and taus. However, the direct neutrino interactions form an important contribution because the neutrino flux at IceCube depths is two orders of magnitude larger than the flux of the secondary charged leptons.

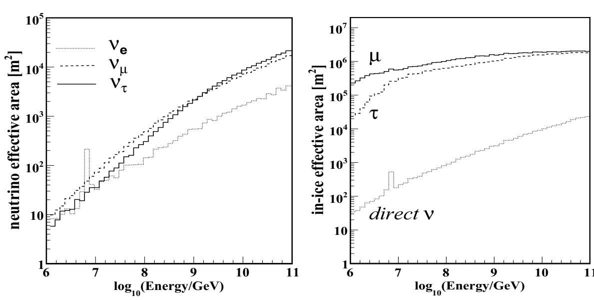

Figure 4: The left panel shows 4π solid angle averaged neutrino effective areas for each neutrino flavor. The dashed line corresponds to $\nu_e+\bar{\nu}_e$. The solid line is $\nu_\mu+\bar{\nu}_\mu$, and the dotted line is $\nu_\tau+\bar{\nu}_\tau$. All assume equal flux of neutrinos and anti-neutrinos. The right panel shows the effective detection area near the detector for secondary muons, taus and primary all flavor neutrinos.

4 Discussions

IceCube may be the first experiment to probe the cosmological evolution of the cosmic-ray sources [19].

While models of astronomical neutrinos include uncertainties in the photon field the cosmic rays interact with prior to escape from sources, CMB induced cosmogenic neutrino models are not affected by this uncertainty. Instead, these neutrino fluxes are highly dependent on the

	model parameters				Event rates
Models	m	Z_{max}	γ	E_{max}	IceCube 1 year
ESS Ω_Λ=0.7 [10]	SFR [18]	-	2.0	10^{22} eV	0.85 ± 0.01
YT [8]	4	4	2.0	10^{22} eV	1.05 ± 0.01
Kalashev *et al.* [9]	5	2	2.0	10^{22} eV	1.65 ± 0.01
Ahlers *et al.* dip transit at 10^{19} eV (best) [11]	4.6	2	2.5	10^{21} eV	0.80 ± 0.01
Ahlers *et al.* dip transit at 10^{19} eV (max.) [11]	4.4	2	2.1	10^{21} eV	1.69 ± 0.01

Table 1: Expected numbers of events by IceCube in 365 days from several cosmogenic neutrino models assuming the cosmic-ray primaries to be protons. The spectral indices γ, cutoff energies E_{max} at sources as well as cosmological evolution indices m and extensions in redshift Z_{max} for the cosmic-ray sources are also listed for reference. The corresponding expected number of background events in one year is 0.11 ± 0.01. Errors are statistical only.

cosmological distributions of the cosmic-ray sources, the cosmic-ray energy spectra in the sources, and the cosmic-ray composition. However, the cosmogenic neutrino event rates expected in IceCube are relatively stable under different assumptions on the spectra injected at the cosmic-ray sources, such as the maximum proton energy at sources and spectral indexes. Reference [9] shows that the neutrino flux significantly increases with decreasing primary spectral index from 2 to 1 only in the energy region above 10^{18} GeV. It is also shown in Ref. [10] that when the spectral index increases to 3, the neutrino spectrum is shifted to a slightly lower energy region. For both cases, only a slight increase in the event rates is expected since the target neutrino energies of IceCube are below $10^{18.5}$ eV [5]. Similarly the dependence on E_{max} is weak because it mainly affects the flux shape above 10^{18} GeV [9]. Therefore IceCube is sensitive to the redshift evolution of the co-moving density of sources, often parametrized with an exponential index m as $(1+z)^m$, to include the redshift dependence.

Studies of the baseline capability of the IceCube detector for cosmogenic neutrinos in the energy region above 1 PeV have shown that IceCube is able to detect cosmogenic neutrinos or constrain fluxes with moderate parameters, m = 3.5 $\sim$ 4.

In this paper we only considered the case of pure proton cosmic-ray primaries for GZK neutrino production. A detector with an order of magnitude larger fiducial volume than IceCube, such as the next generation radio Cherenkov detector arrays, ARA [20] and ARIANNA [21], is required for measurements of neutrino fluxes induced by iron-dominated cosmic-rays.

This is a performance study based on the method already realized and applied to the actual experimental data analysis [5]. New techniques are being developed for future analyses [22, 23]. For example, there is a technique to experimentally identify atmospheric muon bundle events by looking for a coincidence signature in the IceCube optical modules and the IceTop air shower surface array [22]. Differences in the energy loss profiles and waveform shapes between the atmospheric muon bundles and neutrino-induced single muon events are also being explored. These new techniques should improve sensitivities for future cosmogenic neutrino analyses with IceCube.

References

[1] K. Greisen, Phys. Rev. Lett., 1966, **16**, 748.

[2] G. T. Zatsepin and V. A. Kuzmin, Pisma Zh. Eksp. Teor. Fiz., 1966, **4**, 114 [JETP. Lett., 1966, **4**, 78].

[3] V.S. Berezinsky and G.T. Zatsepin, Phys. Lett. B, 1969, **28** 423.

[4] H. Kolanoski, IceCube summary talk, these proceedings.

[5] R. Abbasi *et al.* (IceCube Collaboration) Phys. Rev. D, 2011, **83**, 092003.

[6] D. Heck *et al.*, Report FZKA, 1998, **6019**, Forschungszentrum Karlsruhe.

[7] E. J. Ahn, R. Engel, T. K. Gaisser, P. Lipari, and T. Stanev, Phys. Rev. D, 2009, **80**, 094003.

[8] S. Yoshida and M. Teshima, Prog. Theor. Phys. 1993, **89**, 833.

[9] O. E. Kalashev, V. A. Kuzmin, D. V. Semikoz, and G. Sigl, Phys. Rev. D, 2002, **66**, 063004.

[10] R. Engel, D. Seckel, and T. Stanev, Phys. Rev. D, 2001, **64**, 093010.

[11] M. Ahlers *et al.*, Astropart. Phys. 2010, **34**, 106.

[12] S. Yoshida *et al.*, Phys. Rev. D, 2004, **69**, 103004.

[13] J. Abraham *et al.* (Pierre Auger Collaboration), Phys. Rev. D, 2009, **79**, 102001. Private communications.

[14] I. Kravchenko *et al.* (Rice Collaboration), Phys. Rev. D, 2006, **73**, 082002.

[15] P. W. Gorham *et al.* (ANITA Collaboration), Phys. Rev. D, 2010, **82**, 022004; arXiv:1011.5004 (erratum).

[16] R. Abbasi *et al.* (IceCube Collaboration), Phys. Rev. D, 2010, **82**, 072003.

[17] E. Waxman and J. Bahcall, Phys. Rev. D, 1998, **59**, 023002; S. Razzaque, P. Meszaros, and E. Waxman. Phys. Rev. D, 2003, **68**, 083001.

[18] B.J. Boyle and R.J. Terlevich, Mon. Not. R. Astron. Soc., 1998, **293**, L49-L51.

[19] S. Yoshida and A. Ishihara, paper 954, these proceedings.

[20] P. Allison *et al.*, 2011, arXiv:1105.2854

[21] L. Gerhardt *et al.*, Nucl. Instrum & Meth., 2010, **A624**, 85.

[22] J. Auffenberg, S. Cohen and K. Mase, paper 778, these proceedings.

[23] H. Wissing *et al.*, paper 949, these proceedings.